In-Plane Optical Absorption and Free Carrier Absorption in Graphene-on-Silicon Waveguides

Zhenzhou Cheng, *Graduate Student Member, IEEE*, Hon Ki Tsang, *Senior Member, IEEE*, Xiaomu Wang, *Member, IEEE*, Ke Xu, *Graduate Student Member, IEEE*, and Jian-Bin Xu, *Senior Member, IEEE*

***Abstract*—We experimentally study the in-plane optical absorption and free carrier absorption (FCA) in graphene-on-silicon waveguides using a pump-probe measurement over microsecond timescales. The silicon waveguide is fabricated using complementary metal–oxide–semiconductor compatible processes, and directly covered by a graphene layer. Saturable absorption in the graphene is observed at the beginning of the pump pulse followed by an increase in absorption. The increase in absorption builds up over several microseconds, and is experimental evidence that free carriers generated by the pump absorption in graphene can transfer into silicon waveguides. The FCA in silicon waveguides eventually dominates the optical loss, which reaches ∼9 dB, after several microseconds. All-optical modulations of the probe light are thus demonstrated. There is also a large thermally induced change in waveguide effective refractive index because of the optical absorption in the graphene.**

***Index Terms*—Graphene, free carrier absorption, nonlinear optics, integrated optics, silicon on insulator (SOI) technology, silicon photonics.**

I. Introduction

GRAPHENE with its zero band gap [1], [2], large mobility [3], and linear electron/hole dispersion [4], has been suggested as a promising optoelectronic and optical nonlinear material. It has been used in mode-locking lasers [5]–[7], four-wave mixing wavelength conversions [8], [9], broadband electroabsorption modulators [10], [11], ultrafast photoreceivers [12]–[15], and terahertz-wave generations [16]. However, for traditional normal incident applications [7], [9], [12], [13], [17] the light interaction length is limited by the graphene monolayer thickness (∼0.7 nm) [18]–[20]. Therefore, recent studies have turned their attention to the evanescent field interaction between an optical waveguide and graphene [9]–[11], [17], [21], since the interaction length can be dramatically increased by many orders of magnitude, as shown in Fig. 1(a).

Silicon suspended membrane waveguides (SMWs), coupled by focusing subwavelength gratings, have been proposed and demonstrated for applications from near-infrared (near-IR) to mid-IR [22], [23]. The 2-D nature of graphene makes it very suitable for integration with silicon planar lightwave circuits (PLCs). So graphene-on-silicon suspended membrane PLCs offer the potential for ultrabroadband applications from 1.2 to 8.0 μm. Moreover, it is possible to use complementary metal–oxide–semiconductor compatible processes to fabricate silicon devices, transfer or deposit the graphene onto the silicon and pattern the graphene [24]. The linear absorption associated with

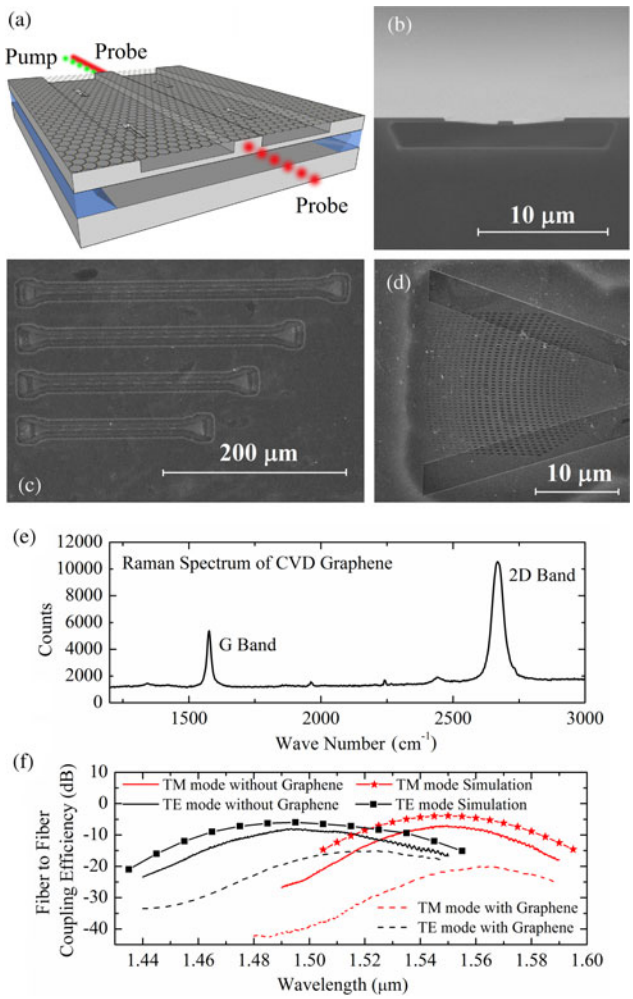

Fig. 1. (a) Schematic illustration of the in-plane pump-probe experiment. (b) SEM image of the cross section of SMW. (c) SEM image of graphene-on-silicon SMWs. (d) SEM image of the grating coupler with graphene on top. (e) Raman spectrum of the graphene on grating coupler which confirms the graphene is monolayer. (f) Transmission measurements of silicon SMWs with and without the graphene on top.

Manuscript received March 15, 2013; revised April 11, 2013 and May 7, 2013; accepted May 7, 2013. Date of publication May 29, 2013; date of current version August 14, 2013. This work was supported in part by the University Grants Committee special equipment under Grant SEG CUHK-01 and Hong Kong Research Grants Council (RGC) GRF under Grants 416512 and 417910. The work of Z. Cheng was supported by the Hong Kong RGC Ph.D. Fellowship.

The authors are with the Department of Electronic Engineering, The Chinese University of Hong Kong, Shatin, Hong Kong (e-mail: acheng@ee.cuhk.edu.hk; hktsang@ee.cuhk.edu.hk; xmwang@ee.cuhk.edu.hk; kxu@ee.cuhk.edu.hk; jbxu@ee.cuhk.edu.hk).

Color versions of one or more of the figures in this paper are available online at http://ieeexplore.ieee.org.

Digital Object Identifier 10.1109/JSTQE.2013.2263115

excitation of electrons from the graphene valence band to the conduction band has been reported in a transverse-electric (TE) mode hydrogen silsesquioxane cladding silicon waveguide with the graphene on top [25]. Optical modulation of the transverse-magnetic (TM) mode in an Al_2O_3 cladding silicon waveguide by applying a voltage to tune the graphene Fermi level has also been reported [10]. Four-wave mixing wavelength conversion has been also demonstrated in a highly p-doped graphene (moving the Fermi position deep into the valence band which can reduce the graphene optical absorption) on a photonic crystal resonator [9]. Understanding the in-plane interaction of propagating light in silicon waveguides with the graphene on top is important for the design and optimization of graphene-on-silicon devices. Although graphene absorption properties have been widely studied for the light of normal incidence [26]–[31]; there is little experimental attention on the in-plane absorption study of graphene-on-silicon waveguides.

In this paper, we experimentally study the in-plane optical absorption of graphene-on-silicon SMWs. A pump-probe experiment is carried out to investigate the dynamic absorption and the carrier transport using a continuous wave (CW) probe and modulated pump. Saturable absorption is observed at the beginning of the pump pulse. The free carriers generated by pump absorption in the graphene can cross into the silicon waveguide and accumulate within a 5 μs pump pulse. Free carrier absorption (FCA) dominates the waveguide loss after microsecond timescales. A large thermally induced change in the effective refractive index (RI) of graphene-on-silicon SMWs is also observed.

II. Devices Design and Fabrications

The SMWs were designed and fabricated on a commercial silicon-on-insulator (SOI) wafer (SOITEC, Inc.), which had 340 nm top silicon layer and 2.0 μm thick buried oxide, as shown in Fig. 1(b). An apodized focusing subwavelength grating was used to couple the light into a 150 μm long fundamental mode SMW at 1.55 μm. The fabrication processes of SMW and grating couplers were described in the references [21], [22]. The grating performance was characterized by a tunable laser, and a fiber polarization controller was employed to change the polarization. The grating couplers had a peak coupling efficiency of –3 dB for TM mode. With the same grating, the maximum coupling efficiency for TE mode was measured to be –4 dB. A commercial graphene sheet, which was chemical vapor deposition grown on a copper foil, was purchased from Graphene Laboratories, Inc. A thin polymethyl methacrylate (PMMA) layer was spin coated over the graphene layer, and the copper was removed by the ammonium persulfate wet etching. The graphene supported by PMMA was rinsed by the deionized water, and wet transferred to SMWs. Finally, the PMMA was removed by acetone. The suspended membrane structure is optimized as described in the reference [22], and no damage of silicon waveguides has been observed during the graphene transfer process. Unlike previous works [10], [24], here we placed a graphene layer directly on silicon waveguides without any planarization or insulator layer. The scanning electron microscope (SEM) images of the graphene-on-silicon SMWs and grating couplers are shown in Fig. 1(c) and (d). The monolayer graphene was identified by Raman spectroscopy which yielded a symmetric 2-D peak at 2671 cm^{-1} with full width at half maximum of 42.7 cm^{-1} and G-to-2-D peak intensity ratio (< 0.5) [32], as shown in Fig. 1(e).

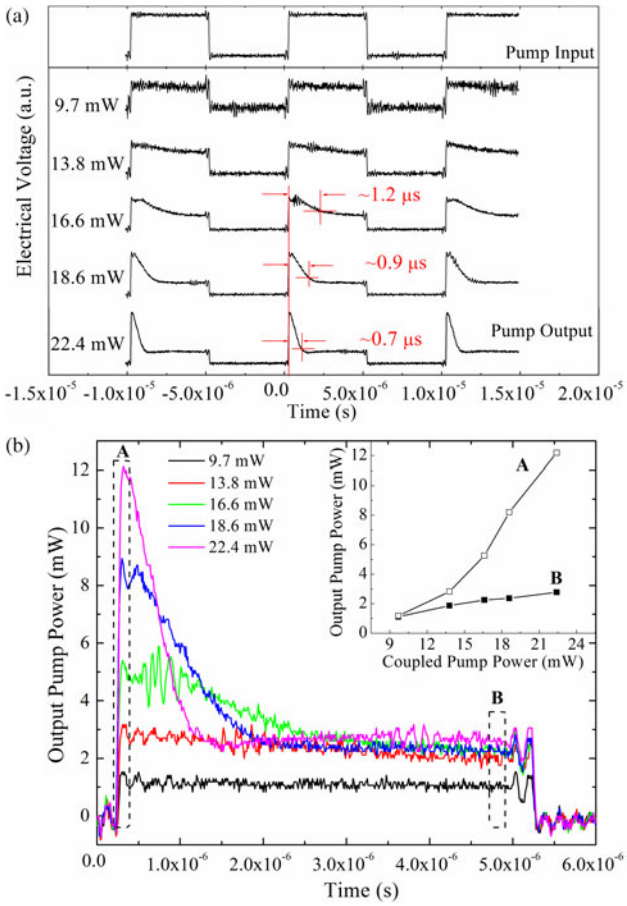

Fig. 2. (a) Pump output power at 100 kHz at different input powers. (b) Pump output power of graphene-on-silicon SMWs. The insert shows the pump output power at the beginning (A) and the end (B) of the pump pulse.

III. Experimental Measurements and Discussions

At low power inputs (< 0.1 mW), the graphene layer introduces a polarization dependent loss, with the TM mode having a larger excess optical loss than the TE mode, as shown in Fig. 1(f). To study the dynamics of the optical absorption of graphene-on-silicon SMWs, we employed a TE mode pump which was modulated by a square wave at 100 kHz using an electrooptic modulator. The modulated pump and a CW TE mode probe (coupled power < 1 mW) were measured at different average pump powers using a 20 GHz photodiode. The pump and probe had wavelengths of 1.55 and 1.56 μm, respectively. The temporal profiles of the pump (no probe) transmission were first measured as shown in Fig. 2(a). Near the start of the pump pulse (A), the pump power showed saturable absorption which was similar to the previous measurement of saturable absorption for the light of normal incidence to the graphene [5]–[7]. In addition to the saturable absorption, we also observed an opposite

increase in the pump absorption, with the rise over a timescale of microseconds. The rise time of the absorption decreased at higher pump powers. After several microseconds (B), the pump loss became almost constant, with a maximum transmission loss of ~13 dB as shown in Fig. 2(b). The time dependence of the observed optical transmission may be explained in terms of an initial saturable absorption in graphene followed by increasing FCA in the silicon waveguide. The FCA was confirmed experimentally to come from the transfer of photoexcited electrons from the graphene to silicon SMWs, since no similar FCA loss was observed in the 150 μm long silicon waveguide without the graphene on top in the experiment. Photoexcited carriers crossing from graphene into silicon has previously been reported in graphene-silicon Schottky diodes [33]. The pump loss mainly includes the electron interband excitation in the graphene and the FCA loss in silicon waveguides. At the steady state (B), the FCA loss, which was caused by scattering of photons by free carriers in the silicon conduction band, dominated the waveguide loss, as shown in Fig. 2(b). The FCA loss can be experimentally estimated by the probe light measurement.

When the pump was switched ON, the probe was modulated by the pump light with a maximum modulation depth of ~87.5%, and the probe had a similar pump-power dependent loss. When the coupled pump power was increased from 9.7 to 22.4 mW, the observed rise time of probe absorption decreased from ~2.2 to ~0.7 μs, as shown in Fig. 3(a) and (b). After the pump was switched OFF, the probe recovered to its original loss in ~1.8 μs, which was almost independent of pump excitation level. The probe recovery time was also consistent with the free carrier lifetimes in silicon, and was much slower than the lifetimes of free carriers in the graphene (picoseconds timescales) [28].

Under a coupled power of 22.4 mW, the pump power absorption is plotted by subtracting the output power (red solid line) from the input power (black dash line), as shown in Fig. 4(a). If the waveguide scattering loss is neglected, which is reasonable because of the high confinement of optical mode in the silicon SMW and the short waveguide length (150 μm), the pump absorption mainly includes the FCA in silicon waveguides and the graphene absorption (associated with interband excitation in the graphene). It is not easy to accurately separate the FCA from the total pump absorption due to the distributed free carrier population in silicon waveguides. Here, we provide a simple model to describe the dynamic absorption in graphene-on-silicon waveguides.

The FCA loss is estimated from the probe modulation experiment. This assumption is reasonable. Although more free carriers will be introduced to the silicon waveguide when the pump power is increased, with the same pump input the FCA loss should be the same for both pump and probe, due to the same carrier density in silicon waveguides. The FCA dominates the waveguide loss in the probe modulation. So the graphene absorption can be calculated from Fig. 4(b), by subtracting the FCA (red solid line) from the total pump absorption (black dash line). Fig. 4(c) shows the graphene absorption. At the beginning of the pump pulse, the graphene absorption dominates the optical absorption, because few electrons have accumulated in

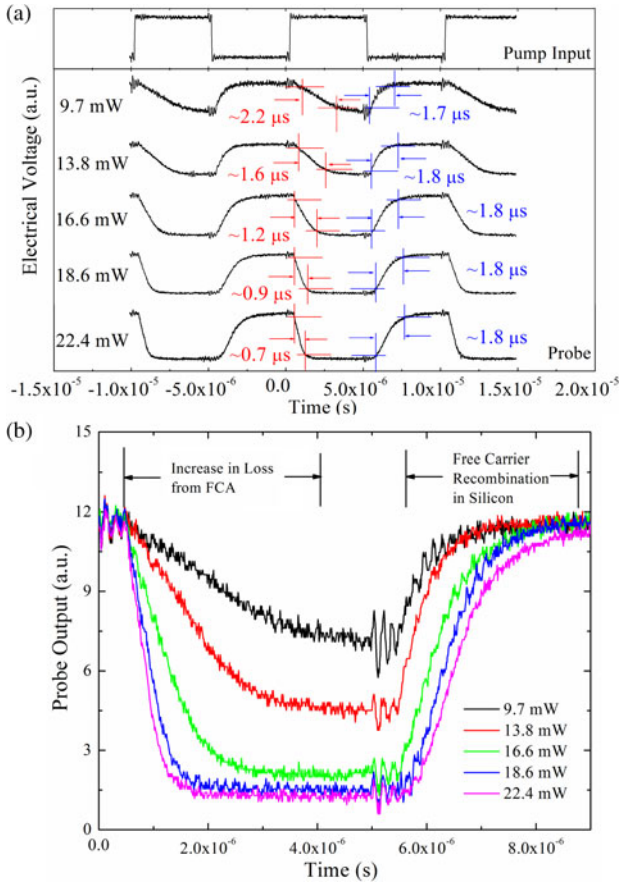

Fig. 3. (a) Temporal response of the CW probe to the modulated pump-probe scheme at 100 kHz. (b) Probe output of the graphene-on-silicon SMW at different pump inputs.

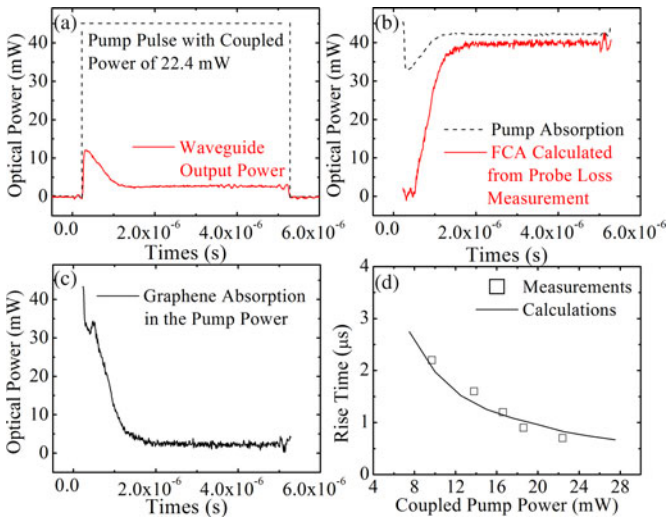

Fig. 4. (a) Coupled pump power and output pump power in one pulse. (b) Pump absorption and FCA from probe measurements in one pulse. (c) Graphene absorption (d) Calculations and measurements of the rise time of the optical absorption in the graphene-on-silicon SMW at different pump powers.

silicon waveguides. As the population of free carriers builds up in silicon waveguides, FCA becomes significant and can dominate the waveguide loss at the end of the pump pulse, as shown

in Fig. 3(b). By integrating the curve in Fig. 4(c), photoexcited electrons are calculated as 4.0×10^{11} over the 5 μs of the pump pulse, by assuming that each absorbed photon generates a free electron-hole pair. The build-up of electrons in silicon SMWs will establish an electric field which will eventually limit the transfer of electrons from the graphene to silicon waveguides. There will also be carrier–carrier scattering loss and recombination processes which will reduce the carrier population [34]. Therefore, only a small fraction of electrons can cross into silicon waveguides, and induce the FCA to the propagating light. The population of free carriers in silicon waveguides that can account for the observed loss may be calculated from [35]:

$$\Delta\alpha = \Delta\alpha_e + \Delta\alpha_h = 8.5\times10^{-18}\times \mathrm{N}_e + 6.0\times10^{-18}\times N_h \quad (1)$$

where $\Delta\alpha_e$ and $\Delta\alpha_h$ are the changes in the absorption resulting from the changes in free-electron (N_e) and free-hole (N_h) carrier concentrations. So the electron population in silicon waveguides is calculated as 2.3×10^9 in the steady state. The electron population in the silicon waveguide may be described by the following rate equation:

$$\frac{dN_e(t)}{dt} = \frac{\eta P_0 e^{\Delta\alpha L}}{h\nu} - \frac{N_e(t)}{\tau} \quad (2)$$

where $N_e(t)$ is the electron density in silicon waveguide, h is the plank constant, ν is the frequency of pump light, τ is the free carrier life time in the silicon waveguide which is measured as $\sim$1.8 μs in the pump-probe experiment, L is the waveguide length (150 μm), $\Delta\alpha$ is the free carrier introduced waveguide loss which depends on the $N_e(t)$ in the silicon waveguide, P_0 is the coupled pump power. η indicates the conversion efficiency from the pump light photon to the electron in the silicon waveguide, which is also associated with the pump power and electron density in the silicon waveguide, because the building-up electron density may increase the electrical barrier between the silicon and the graphene. For simplicity, we just estimate the average conversion efficiency from the electron population in silicon waveguide and the photoexcited electron in graphene. Fig. 4(d) compares the calculated rise times of the optical absorption at different pump power levels with the measured rise times in Fig. 3(a). The theoretical calculation basically agrees with the experimental measurement.

We also carried out a CW pump-probe experiment to measure the real part change of the effective RI of graphene-on-silicon waveguides. The pump was coupled with TE mode polarization, and the output power of TE and TM mode probes were measured at different pump powers, as shown in Fig. 5. The Fabry–Perot (F–P) oscillations, with a free spectral range (FSR) of $\sim$1.5 nm ($\sim\pi$ phase shift), were produced by the grating back reflection, and allowed us to obtain the changes in the real part of the effective RI of graphene-on-silicon SMWs. As a control experiment, we performed the same measurement on silicon waveguides without any graphene on top, as shown in Fig. 5(a). We observed only a small (0.6 dB) intensity dependence that may be attributed to the free carriers generated by the two photon absorption (TPA) in a 150 μm long silicon waveguide; the TPA in silicon will be even smaller in graphene-on-silicon

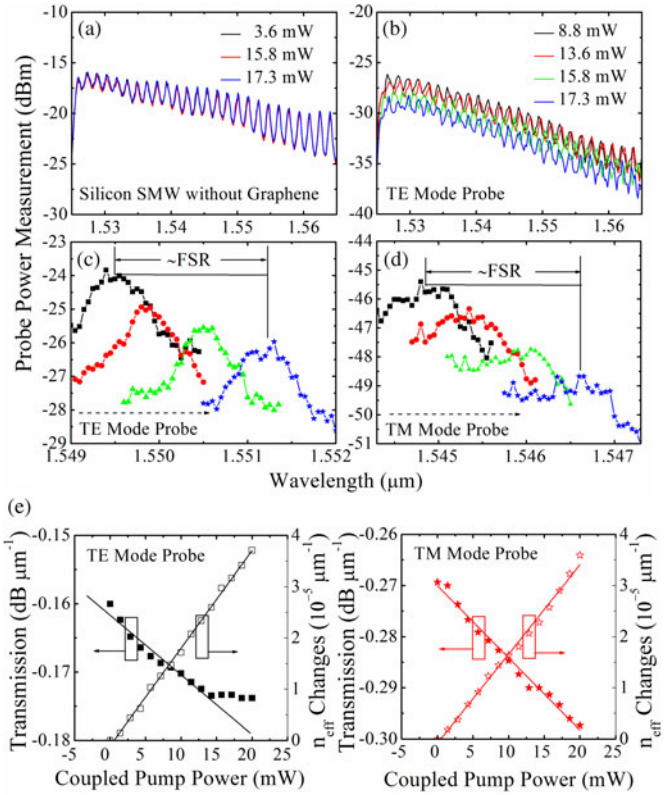

Fig. 5. (a) TE mode probe measurements of silicon SMWs without the graphene on top under different pump powers. (b) TE mode probe measurements of graphene-on-silicon SMWs under different pump powers. (c) TE mode probe measurements of the graphene-on-silicon SMWs under four different pump powers (0, 4.3, 10, and 15.7 mW). (d) TM mode probe measurements of the graphene-on-silicon SMWs under four different pump powers (0, 5.7, 11.5, and 17.2 mW). The dash lines indicate the F–P shift with increasing the pump power. (e) The graphene-on-silicon SMW transmission and measured changes of effective RI under different pump powers.

SMWs because of the lower pump power. No wavelength shift of F–P oscillations was observed in bare silicon waveguides. However, for the graphene-on-silicon SMW, a much larger intensity dependence of the probe light spectrum was observed, as shown in Fig. 5(b). The probe F–P oscillations shifted to longer wavelength with increasing pump powers. The observed red shifts of F–P oscillations implied the presence of a large linear change of the effective RI. Large changes in the effective RI were consistent with thermal-optic effects. The absorption of pump power increased the free carrier density in the graphene. In the steady state, the relaxation of free carriers will eventually produce a temperature rise in silicon SMWs since the air cladding of SMWs provided a good thermal isolation. This observation is different from the blue-shift observed in graphene excited at the normal incidence [34], because free carriers in the graphene layer will introduce a temperature rise that introduces an effective RI increase that is larger than the decrease from plasma dispersion effect in the silicon waveguide. The graphene layer suffered irreversible thermal damage, when the coupled power approached $\sim$30 mW. From F–P shifts, the waveguide temperature rise was calculated to be $\sim$20.7 K at the coupled pump power of 15.7 mW, which produced a shift of

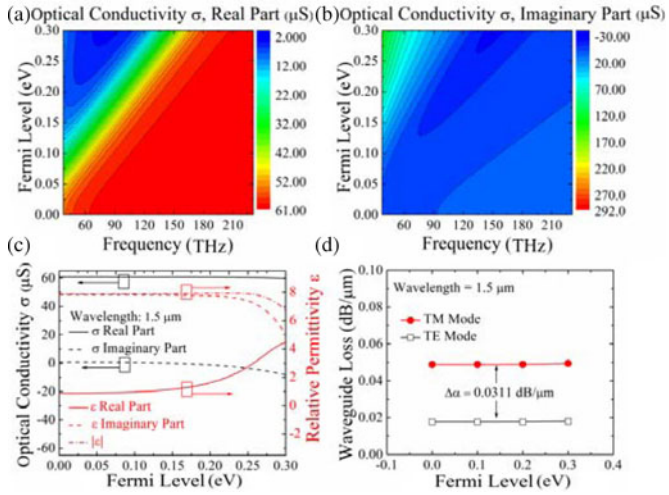

Fig. 6. (a) Real part and (b) Imaginary part of the graphene optical conductivity as a function of the Fermi level and light frequency (temperature: 300 K, scattering rate: 5 meV), following the Kobo formula. (c) Graphene optical conductivity and effective relative permittivity as a function of Fermi level at 1.5 μm. (d) Theoretical optical loss of graphene-on-silicon SMWs under four different Fermi levels for two polarizations.

about one FSR ($\sim\pi$ phase shift), as shown in Fig. 5(c) and (d). Although the effective IR changes were similar for two polarizations under different pump powers, the graphene-on-silicon waveguide showed polarization-dependent probe transmission as described in Fig. 5(e). We observed an increasing loss in the TE mode, with increase saturating at 15 mW, but the TM mode loss does not saturate even at the coupled pump power of 20 mW. The modulation coefficients were 8.72×10^{-4} and 14.1×10^{-4} dB/μm/mW for TE mode and TM mode probes, respectively. With high intensity pumps, the TM mode probe shows larger excess loss than TE mode. The reason may be explained by the different optical loss of graphene-on-silicon SMWs with two polarizations, which can be estimated numerically.

The optical conductivity σ describes the optical absorption of graphene, and can be computed from the Kubo formalism [2], [17]. σ include the contributions from intraband and interband transmissions: $\sigma = \sigma_{\text{intra}}(\omega) + \sigma_{\text{inter}}(\omega)$ [36], [37]. In our experiment, the pristine graphene was employed without deliberate doping. The real part and imaginary part of graphene optical conductivity as a function of the Fermi level and light frequency were calculated with a low Fermi level, as shown in Fig. 6(a) and (b). Then, the effective relative permittivity ε_{eff} of graphene is given by the following formula [10], [11]:

$$\varepsilon_{\text{eff}} = 1 + i\frac{\sigma}{\omega\varepsilon_0\Delta} \tag{3}$$

where the ε_0 is the vacuum permittivity, and Δ is the graphene effective thickness, taken to be 0.7 nm in the simulation [10], [11]. At 1.5 μm wavelength, the optical conductivity and effective relative permittivity were calculated as shown in Fig. 6(c). For graphene-on-silicon SMWs, propagating light is mainly confined by the RI step between silicon and air, with a graphene layer perturbation. Based on above theoretical parameters, the TE_{11} and TM_{11} modes of graphene-on-silicon SMWs were simulated at 1.5 μm wavelength using the effective index method by the commercial finite element method software (COMSOL Multiphysics). The theoretical losses can be calculated by the imaginary part of waveguide effective RI, as shown in Fig. 6(d). The attenuation of TM mode was obviously larger than TE mode.

IV. Conclusion

In summary, we report the experimental study of in-plane optical absorption of graphene-on-silicon waveguides. Our measurements show that free carriers produced by evanescent field optical absorption in the graphene layer can transfer into the silicon waveguide and accumulate there to give rise to FCA losses. The total optical loss from both the FCA and the graphene absorption can reach $\sim$13 dB, and may be used to modulate the probe power. Relaxation of hot carriers in the graphene layer can lead to a temperature rise in the graphene which can change the real part of waveguide effective RI by the thermal-optic effect. The results in this work may help to design and optimize graphene-on-silicon devices.

References

[1] I. Meric, M. Y. Han, A. F. Young, B. Ozyilmaz, P. Kim, and K. L. Shepard, "Current saturation in zero-bandgap, top-gated graphene field-effect transistors," *Nature Nanotechnol.*, vol. 3, pp. 654–659, Sep. 2008.

[2] A. H. C. Neto, F. Guinea, N. M. R. Peres, K. S. Novoselov, and A. K. Geim, "The electronic properties of graphene," *Rev. Mod. Phy.*, vol. 81, pp. 109–162, Jan. 2009.

[3] F. Bonaccorso, Z. Sun, T. Hasan, and A. C. Ferrari, "Graphene photonics and optoelectronics," *Nature Photon.*, vol. 4, pp. 611–622, Sep. 2010.

[4] S. A. Mikhailov, "Non-linear electromagnetic response of graphene," *Europhys. Lett.*, vol. 79, no. 2, p. 27002, Jul. 2007.

[5] L. Gui, W. Zhang, X. Li, X. Xiao, H. Zhu, K. Wang, D. Wu, and C. Yang, "Self-assembled graphene membrane as an ultrafast mode-locker in an erbium fiber laser," *IEEE Photon. Technol. Lett.*, vol. 23, no. 23, pp. 1790–1792, Dec. 2011.

[6] Q. Bao, H. Zhang, Y. Wang, Z. Ni, Y. Yan, Z. X. Shen, K. P. Loh, and D. Y. Tang, "Atomic-layer graphene as a saturable absorber for ultrafast pulsed lasers," *Adv. Funct. Mater.*, vol. 19, pp. 3077–3083, 2009.

[7] Z. Sun, T. Hasan, F. Torrisi, D. Popa, G. Privitera, F. Wang, F. Bonaccorso, D. M. Basko, and A. C. Ferrari, "Graphene mode-locked ultrafast laser," *ACS Nano*, vol. 4, no. 2, pp. 803–810, Jan. 2010.

[8] T. Gu, N. Petrone, J. F. McMillan, A. V. D. Zande, M. Yu, G. Q. Lo, D. L. Kwong, J. Hone, and C. W. Wong, "Regenerative oscillation and four-wave mixing in graphene optoelectronics," *Nature Photon.*, vol. 6, pp. 554–559, Aug. 2012.

[9] B. Xu, A. Martinez, and S. Yamashita, "Mechanically exfoliated graphene for four-wave-mixing-based wavelength conversion," *IEEE Photon. Technol. Lett.*, vol. 24, no. 20, pp. 1792–1794, Oct. 2012.

[10] M. Liu, X. Yin, E. Ulin-Avila, G. Geng, T. Zentgraf, L. Ju, F. Wang, and X. Zhang, "A graphene-based broadband optical modulator," *Nature*, vol. 474, pp. 64–67, Jun. 2011.

[11] M. Liu, X. Yin, and X. Zhang, "Double-layer graphene optical modulator," *Nano Lett.*, vol. 12, pp. 1482–1485, Feb. 2012.

[12] T. Mueller, F. Xia, and P. Avouris, "Graphene photodetectors for high-speed optical communications," *Nature Photon.*, vol. 4, pp. 297–301, May 2010.

[13] F. Xia, T. Mueller, Y. Lin, A. Valdes-Garcia, and P. Avouris, "Ultrafast graphene photodetector," *Nature Nanotechnol.*, vol. 4, pp. 839–843, Dec. 2009.

[14] D. Sun, G. Aivazian, A. M. Jones, J. S. Ross, W. Yao, D. Cobden, and X. Xu, "Ultrafast hot-carrier-dominated photocurrent in graphene," *Nature Nanotechnol.*, vol. 7, pp. 114–118, Feb. 2012.

[15] F. Xia, T. Mueller, R. Golizadeh-Mojarad, M. Freitag, Y. Lin, J. Tsang, V. Perebeinos, and P. Avouris, "Photocurrent imaging and efficient photon detection in a graphene transistor," *Nano Lett.*, vol. 9, pp. 1039–1044, Feb. 2009.

[16] T. Otsuji, S. B. Tombet, A. Satou, M. Ryzhii, and V. Ryzhii, "Terahertz-wave generation using graphene: toward new types of terahertz lasers," *IEEE J. Sel. Topics Quantum Electron.*, vol. 19, no. 1, art. no. 8400209, Jan./Feb. 2013.
[17] Q. Bao and K. P. Loh, "Graphene photonics, plasmonics, and broadband optoelectronic devices," *ACS Nano*, vol. 6, no. 5, pp. 3677–3694, Apr. 2012.
[18] F. Wang, Y. Zhang, C. Tian, C. Girit, A. Zettl, M. Crommie, and Y. R. Shen, "Gate-variable optical transitions in graphene," *Science*, vol. 320, pp. 206–209, Apr. 2008.
[19] Z. Q. Li, E. A. Henriksen, Z. Jiang, Z. Hao, M. C. Martin, P. Kim, H. L. Stormer, and D. N. Basov, "Dirac charge dynamics in graphene by infrared spectroscopy," *Nature Phys.*, vol. 4, pp. 532–535, Jul. 2008.
[20] R. R. Nair, P. Blake, A. N. Grigorenko, K. S. Novoselov, T. J. Booth, T. Stauber, N. M. R. Peres, and A. K. Geim, "Fine structure constant defines visual transparency of graphene," *Science*, vol. 320, p. 1308, Jun. 2008.
[21] Q. Bao, H. Zhang, B. Wang, Z. Ni, C. H. Y. X. Lim, Y. Wang, D. Y. Tang, and K. P. Loh, "Broadband graphene polarizer," *Nature Photon.*, vol. 5, pp. 411–415, Jul. 2011.
[22] Z. Cheng, X. Chen, C. Y. Wong, K. Xu, and H. K. Tsang, "Mid-infrared suspended membrane waveguide and ring resonator on silicon-on-insulator," *IEEE Photon. J.*, vol. 4, no. 5, pp. 1510–1519, Oct. 2012.
[23] Z. Cheng, X. Chen, C. Y. Wong, K. Xu, and H. K. Tsang, "Apodized focusing subwavelength grating couplers for suspended membrane waveguides," *Appl. Phys. Lett.*, vol. 101, pp. 101104-1–101104-4, Sep. 2012.
[24] K. S. Novoselov, A. K. Geim, S. V. Morozov, D. Jiang, M. I. Katsnelson, I. V. Grigorieva, S. V. Dubonos, and A. A. Firsov, "Two-dimensional gas of massless Dirac fermions in graphene," *Nature*, vol. 438, pp. 197–200, Nov. 2005.
[25] H. Li, Y. Anugrah, S. J. Koester, and M. Li, "Optical absorption in graphene integrated on silicon waveguides," *Appl. Phys. Lett.*, vol. 101, pp. 111110-1–111110-5, Sep. 2012.
[26] H. Choi, F. Borondics, D. A. Siegel, S. Y. Zhou, M. C. Martin, A. Lanzara, and R. A. Kaindl, "Feasibility of terahertz lasing in optically pumped epitaxial multiple graphene layer structures," *J. Appl. Phys.*, vol. 106, pp. 084507-1–084507-6, Oct. 2009.
[27] D. Sun, Z. Wu, C. Divin, X. Li, C. Berger, W. A. de Heer, P. N. First, and T. B. Norris, "Ultrafast relaxation of excited Dirac fermions in epitaxial graphene using optical differential transmission spectroscopy," *Phys. Rev. Lett.*, vol. 101, pp. 157402-1–157402-4, Oct. 2008.
[28] M. Breusing, S. Kuehn, T. Winzer, E. Malic, F. Milde, N. Severin, J. P. Rabe, C. Ropers, A. Knorr, and T. Elsaesser, "Ultrafast nonequilibrium carrier dynamics in a single graphene layer," *Phys. Rev. B*, vol. 83, pp. 153410-1–153410-4, Apr. 2011.
[29] F. H. L. Koppens, D. E. Chang, and F. J. G. de Abajo, "Graphene plasmonics: A platform for strong light-matter interactions," *Nano Lett.*, vol. 11, pp. 3370–3377, Jul. 2011.
[30] S. Thongrattanasiri, F. H. L. Koppens, and F. J. G. de Abajo, "Complete optical absorption in periodically patterned graphene," *Phys. Rev. Lett.*, vol. 108, pp. 047401-1–047401-5, Jan. 2012.
[31] X. Xu, N. M. Gabor, J. S. Alden, A. M. van der Zande, and P. L. McEuen, "Photo-thermoelectric effect at a graphene interface junction," *Nano Lett.*, vol. 10, pp. 562–566, Jan. 2010.
[32] X. Li, Y. Zhu, W. Cai, J. An, S. Kim, J. Nah, D. Yang, R. Piner, A. Velamakanni, I. Jung, E. Tutuc, S. K. Banerjee, L. Colombo, and R. S. Ruoff, "Large-area synthesis of high-quality and uniform graphene films on copper foils," *Science*, vol. 324, pp. 1312–1314, Jun. 2009.
[33] C. Chen, M. Aykol, C. Chang, A. F. J. Levi, and S. B. Cronin, "Graphene-silicon Schottky diodes," *Nano Lett.*, vol. 11, pp. 1863–1867, Apr. 2011.
[34] S. Winnerl, F. Göttfert, M. Mittendorff, H. Schneider, M. Helm, T. Winzer, E. Malic, A. Knorr, M. Orlita, M. Potemski, M. Sprinkle, C. Berger, and W. A. de Heer, "Time-resolved spectroscopy on epitaxial graphene in the infrared spectral range-relaxation dynamics and saturation behavior," *J. Phys.: Condens. Matter*, vol. 25, pp. 054202-1–054202-14, Jan. 2013.
[35] G. T. Reed, G. Mashanovich, F. Y. Gardes, and D. J. Thomson, "Silicon optical modulators," *Nature Photon.*, vol. 4, pp. 518–526, Aug. 2010.
[36] S. A. Mikhailov and K. Ziegler, "New electromagnetic mode in graphene," *Phys. Rev. Lett.*, vol. 99, pp. 016803-1–016803-4, Jul. 2007.
[37] J. T. Kim and S. Choi, "Graphene-based plasmonic waveguides for photonic integrated circuits," *Opt. Express*, vol. 19, pp. 24557–24562, Nov. 2011.

Zhenzhou Cheng (S'11) received the B.S. and M.S. degrees in physics from Nankai University, Nankai, Tianjin, China, in 2006 and 2009, respectively. He is currently working toward the Ph.D. degree in the Department of Electronic Engineering, the Chinese University of Hong Kong, Hong Kong. He won the Hong Kong Research Grant Council Ph.D. Fellowship Award in 2010–2013. His current research interests include the silicon-on-sapphire and suspended membrane waveguides for mid-infrared silicon photonics and graphene-on-silicon devices.

Hon Ki Tsang (M'91–SM'04) received the Bachelor of Arts (Hons.) degree in electrical and information sciences engineering and the Ph.D. degree from the University of Cambridge. In 1990 and 1993, he was a Research Visitor at Bellcore (Redbank, NJ, USA). He was also a Postdoctoral Fellow at the School of Physics, University of Bath in the early 1990s. He joined the Chinese University of Hong Kong in 1993 as a Lecturer. From 2002 to 2003, he worked at Bookham Technology plc (U.K.) as the R&D Director, heading the development of multichannel silicon variable optical attenuators, optical channel monitors, and integrated optical transceivers. He returned to the Chinese University of Hong Kong in 2003 and he has been the Head of the Department of Electronic Engineering since 2010. He has published more than 280 papers in journals and conference proceedings. His research interests include silicon photonics since 2000.

Xiaomu Wang (S'07–M'09) received the Ph.D. degree from the Department of Electronic Engineering, the Chinese University of Hong Kong, HKSAR, China, in 2012. He is currently a Postdoctoral Research Fellow in the same department. He won the Young Scientist Award from Hong Kong Institute of Science in 2012. His current research interests include the graphene-based nanoelectronic and nanophotonic devices.

Ke Xu (S'12) received B.Eng. degree from Hua Zhong University of Science and Technology, Wuhan, China, in 2010. He is currently working toward the Ph.D. degree in the Department of Electronic Engineering, The Chinese University of Hong Kong, Shatin, Hong Kong.

Jian-Bin Xu (M'95–SM'02) received the B.Sc. and M.Sc. degrees in physics and information physics from Nanjing University, Nanjing, China, in 1983 and 1986, respectively, under the supervision of S.-Y. Zhang (Member of Chinese Academy of Sciences). Since 1988, he was highly privileged to study in the University of Konstanz (an elite university), particularly under the supervision of K. Dransfeld (Member of German Academy of Sciences). His doctoral dissertation was focused on the near-field sensing and nanoscopic energy transfer and heat transport associated with electronic processes. He earned his doctorate (Dr. rer. nat.) in 1993. Afterward, he joined the Department of Electronic Engineering, The Chinese University of Hong Kong. He has been a Professor in the Department since the mid of 2002. Dr. Xu has published extensively on advanced electronic and photonic materials and devices as well as on nanotechnology in peer-reviewed professional journals (c.a. 220) and conferences (c.a. 50) as well as more than 200 presentations, including conference invited talks, colloquia, seminars, etc. He actively participates in a myriad of professional activities and has served as symposium chair in several international conferences. He is a Fellow of Hong Kong Institution of Engineers, the Secretary and Council Member of Hong Kong Materials Research Society, and a Member of American Physical Society, Materials Research Society, Hong Kong Institution of Science, and Physical Society of Hong Kong.